Vol. 20, No. 1 (2021) 185-194
Revista Mexicana de Ingeniería Química

Influence of retinyl palmitate on nucleation and growth kinetics in batch sugarcane crystallization

Influencia de palmitato de retinilo en las cinéticas de nucleación y crecimiento en la cristalización batch de la caña de azúcar

P.A. Quintana-Hernández*, X.M. Medina-Galván, D. Maldonado-Caraza and J.N. Reyes-Valadez

Departamento de Ingeniería Química. Tecnológico Nacional de México en Celaya. ITC. Antonio García Cubas Pte. # 600 esq. Av. Tecnológico, Celaya, Guanajuato, 38010, México

Received: July 28, 2020; Accepted: August 15, 2020

Abstract

The influence of retinyl palmitate (RP) on nucleation and growth kinetics, in the sugarcane fortification process, is analyzed. Batch crystallization experiments, following natural and linear cooling profiles, were carried out adding different amounts of RP. At each experiment, 10 cm^3 samples were collected every 10 minutes and sugar concentration, crystal mass and crystal size distribution were measured. Nucleation and growth rates were calculated experimentally and kinetic parameters were determined using power-law type relations. At the end of each experiment, crystals were observed in a microscope and morphological changes were analyzed. The results showed that the presence of RP in the fortification process of sugar generated a decrease in both nucleation and growth rates. The decrement was bigger when the initial concentration of RP increased. Moreover, it was observed that fortified crystals suffered morphological changes into their habit.

Keywords: Crystal morphology, kinetics parameters, modelling, nucleation and growth rates, shape factors.

Resumen

En este trabajo se analiza la influencia del palmitato de retinilo (PR) en las cinéticas de nucleación y crecimiento, en el proceso de fortificación del azúcar de caña. Se llevaron a cabo experimentos de cristalización por enfriamiento con perfiles natural y lineal, en un sistema por lotes, añadiendo diferentes cantidades de PR. En cada experimento, se tomaron muestras de 10 cm^3 cada 10 minutos y se midieron la concentración de azúcar, la masa de cristal y la distribución del tamaño de cristales. Las velocidades de nucleación y crecimiento fueron determinadas experimentalmente y los parámetros cinéticos se determinaron utilizando relaciones de tipo ley de potencia. Al final de cada experimento, los cristales fueron observados en un microscopio y se analizaron los cambios morfológicos. Los resultados mostraron que la presencia de PR en el proceso de fortificación de azúcar provocó una reducción en las velocidades de nucleación y crecimiento. Esta disminución fue mayor cuando aumentó la concentración inicial de PR. Además, se observó que los cristales fortificados sufrieron cambios morfológicos en su hábito.

Palabras clave: Morfología de cristales, parámetros cinéticos, modelado, velocidades de nucleación y crecimiento, factor de forma.

1 Introduction

Crystallization is a commonly used separation process that purifies fluids by forming solids. The separation of these two phases is achieved when the physical conditions create supersaturated solutions. Crystallization has been analyzed using different transport mechanisms that involve nucleation and crystal growth. Both mechanisms depend on supersaturation, temperature and interfacial tension. In the crystallization of pure solutions, homogeneous nucleation appears at high supersaturations and in the presence of foreign nuclei heterogeneous nucleation is induced at lower supersaturations (Jones, 2002). Classical nucleation theory provides the background for explaining the nucleation mechanism and includes equations such as the Gibbs-Thompson for homogeneous nucleation (Mullin, 2001) and a modified equation for heterogeneous nucleation that introduce a factor that accounts for the decreased energy barrier to nucleation due to the foreign solid phase (Söhnel and Garside, 1992).

* *Corresponding author. E-mail*: pedro@iqcelaya.itc.mx
Tel. 46-16-62-55-81, Fax 46-16-62-55-57
https://doi.org/10.24275/rmiq/Cat1928
ISSN:1665-2738, *issn-e*: 2395-8472

Moreover, several theoretical models for crystal growth, based on a diffusion and integration process have been proposed (Mullin, 2001). Unfortunately, the theoretical equations include parameters that are not easily measured; so that, nucleation and growth rates are generally evaluated using experimental data and empirical correlational models for every required system (Quintana-Hernandez, *et al*., 2008).

On the other hand, batch cooling crystallization has proved to be an efficient method for sugarcane fortification with Vitamin A using microencapsulated spheres of retinyl palmitate. In this process, RP microspheres adhered to sugar crystal faces or they are encapsulated into the growing sugar crystals. Quintana-Hernandez *et al*. (2020) reported that the retained RP percentage increased with the increase in initial RP concentration. However, the effects of RP on crystallization kinetics and crystal morphological changes are unknown.

In the literature, it has been reported that impurities modify the solubility of a solute in a system depending on the impurities concentration and temperature. Zhang *et al*. (2012) showed that the presence of racemic malic, succinic and citric acids impurities increased the solubility of zinc lactate when increase the impurity concentration. Ugarte *et al*. (1999) determine sucrose solubility with different impurities concentrations of chloride potassium, aspartic acid and tyrosine. Sucrose solubility increases at high KCl concentration but decreases at low KCl concentration. Besides, they reported that sucrose solubility increases in the presence of aspartic acid but decreases in the presence of tyrosine. Contreras and Hernández (2005) evaluated the solubility of sugar cane in presence of different amino acid impurities. They found that solubility decreased with an increment in the impurities concentration. On the other hand, Quintana-Hernández *et al*. (2020) reported a low influence of RP on the solubility of sugarcane at the concentrations analyzed but a high influence of temperature.

Moreover, the presence of impurities induces changes in the nucleation mechanism. Sometimes, impurities reduce the overall free energy change required for critical nucleus formation and enhance heterogeneous nucleation at a lower supersaturation. Mullin (2001) described how small amounts of foreign ions produced an inhibitory effect on nucleation of some inorganic salts. He mentioned that after a threshold ion concentration the inhibitory effects decreased. For other systems, impurities act as nucleation accelerators, and sometimes enhance secondary nucleation when inhibit primary nucleation (Sarig and Mullin, 1982). Kubota (2001) reported that most of the impurities reduced the growth, others enhanced it, and some others stopped it completely. Therefore, there is no way to generalize the overall effect of impurities on nucleation.

Similarly, the effects of impurities on crystal growth cannot been generalized. Zhang *et al*. (2017) showed that the adsorption of foreign particles into active sites generate an increment in interfacial tension, a reduction of crystal growth, and changes in crystal habits. Sgualdino *et al*. (1996) showed that the presence of raffinose during the crystallization of sucrose stopped the growth of some of its crystallographic faces and it produce elongated crystals. Vavrinecz (1965) published an Atlas of Sugar Crystals and showed many different shapes of sucrose crystals generated by the presence of impurities or obtained under different growth conditions. Unfortunately, it has not been possible to establish any relationship between impurities concentration and crystallographic changes. In addition, the influence of RP on crystallization kinetic parameters or possible morphological changes in crystal habit have not been reported in the literature.

Three strategies for evaluating kinetic parameters (base on power-law type equations) have been reported in the literature using the data generated in batch experiments (Qiu and Rasmuson, 1994; Zhang, *et al*., 2017). The first strategy uses direct measurements on individual crystals (Monaco and Rosenberger, 1993); this approach is slow, expensive and not very reproducible. The second one uses experimental measurements of solution concentration, mass of crystals formed and crystal size distribution (CSD) (Wey, 1985). In the third one, the kinetic parameters are determined using an optimization process where population, mass and energy balances are solved minimizing the sum of the squares of the difference between experimental and calculated data of solute concentration (Medina-Galván, *et al*., 2020). This last strategy, sometimes become difficult due to the highly non- lineal behavior of the power-law relations that generate a large number of possible local minimum solutions.

In this work, the effects of RP on the kinetic parameters and crystal morphology were investigated. Cooling crystallization experiments with different RP concentrations were performed. Saturated sugarcane solutions were prepared and supplemented with different RP concentrations. Solutions were cooled following either natural or lineal cooling profiles.

Every 10 minutes a 10 cm^3 sample was analyzed. Sugar concentration, mass of crystals and crystal size distribution were determined. Nucleation and growth rates were evaluated for each sample. Kinetic parameters were determined correlating the experimental results with power-law type models. At the end of each experiment, crystals were filtrated and observed in an optical microscope. With the image processing software developed in this work, characteristic dimensions of some crystals were measured and specific shape factors were calculated. Morphological changes were analyzed based on the physical habit shown and the values of specific shape factors.

2 Experiment

2.1 *Materials and reagents*

Sugar cane obtained from Distribuidora de azúcar (Celaya, Mexico) was purified by recrystallization up to a mass purity of 99.0 wt%. Vitamin-A, as retinyl palmitate powdery with 500,000 IU/g was provided by F. Hoffmann-La Roche (Basel, Switzerland), microspheres (mean of 3.94 μm and a standard deviation of 2.76 μm) were used in this work.

2.2 *Experimental apparatus*

Cooling crystallization experiments were performed in a three-liter stainless steel crystallizer provided with four fixed vertical baffles equally spaced, and a heat exchange jacket. An agitator Janke & Kunkel RW20DZM (Germany) with a double blade connected to an electrical motor provided the necessary agitation in the range of 50-1200 rpm. Sugar concentration (°Brix, g sugar/100 g solution) was measured with an Abbe refractometer Atago DR-A1 (USA). Sugar and RP samples were weighted on an analytical balance Mettler Toledo AG245 (USA) with accuracy (0.01 mg). Temperatures were measured with J-type thermocouples and recorded with a data acquisition equipment cDAQ 9401 (National Instruments, USA). A Huber HS40 (Germany) system was programmed to generate the natural and lineal cooling profiles shown on Fig. 1. Crystal size distributions (CSD) were measured with a Master Sizer S (Malvern Instruments, England).

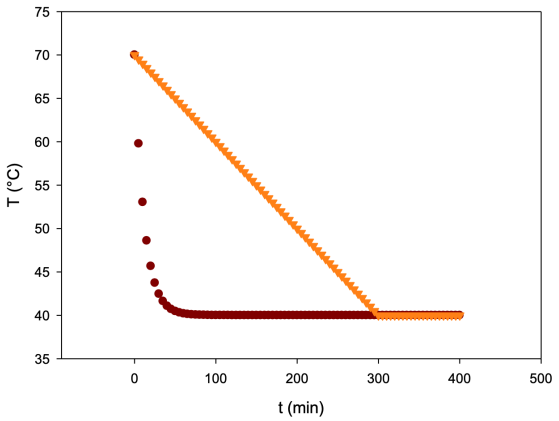

Fig. 1. Experimental temperature cooling profiles, ● natural and ▼ linear.

Crystal habit was observed with an optical microscope Iroscope MG-18 (Mexico) and crystal dimensions were obtained with the image processing software DCA (Mexico) developed in this work.

2.3 *Experimental procedure*

Saturated solutions with 2844 g of sugarcane and the corresponding RP mass for each experiment (see Table 1) were dissolved in 900 cm^3 of water. Solutions were heated above 70 °C during 30 minutes for the complete dissolution of the sugar. Then the solution was cooled. Temperature cooling profiles were selected based on previous reported studies (Quintana-Hernández, *et al.*, 2004; Bolaños *et al.*, 2008; Sánchez-Sánchez, *et al.*, 2017, 2020; Quintana-Hernández, *et al.*, 2020). Natural cooling profiles induce faster supersaturation changes than linear cooling profiles and promote faster mass transfer from the liquid phase to the solid phase. Natural cooling experiments lasted 300 minutes and experiments cooled with lineal profiles continued after 300 minutes at a constant temperature of 40 °C and lasted 400 minutes.

Table 1. Experimental conditions for each run.

Experiment	Profile	RP (g)
E1	Natural	0
E2	Natural	0.4689
E3	Natural	4.6890
E4	Lineal	0
E5	Lineal	0.5121
E6	Lineal	5.1210

To ensure similar mixing conditions and reduce agglomeration, attrition and breakage agitation rate in all experiments was kept constant at 180 rpm. Bolaños *et al*. (2008) reported that in the sugar crystallization process agglomeration appeared at rates below 100 rpm and breakage at rates above 500 rpm. Every 10 minutes, a constant volume sample of 10 cm^3 was taken. The samples were filtered (Whatman 40) and the solution concentration was measured, keeping temperature constant in the refractometer. Crystals were dried under vacuum at room temperatures for 30 minutes and their mass and CSD were determined. At the end of each run, crystals were filtrated, dried and observed in an optical microscope. Crystal characteristic dimensions were determined and crystal habits were compared among pure and fortified crystals.

3 Crystallization kinetics evaluation

3.1 Sugar solubility estimation

Quintana-Hernandez *et al*. (2020) found that RP had no considerable influence on sugar solubility in water due to the microencapsulated RP particles were not soluble in the mixture. Therefore, eqs. (1)-(2) were used to evaluate sugar solubility in this work.

$$A = -0.000701T^2 + 0.264T + 60.912 \tag{1}$$

$$c_s = \left(\frac{A}{100 - A}\right) \tag{2}$$

where A is the sugar saturation concentration measured in °Brix and c_s is the sugar saturation concentration given in g of sugar/cm^3 water. T is the saturation temperature (°C). Equation (1) is valid in the range of 20 to 85 °C and it has a coefficient of determination $R^2 = 0.9902$.

3.2 Kinetic parameters estimation

The solution concentration was estimated using Eq. (3) where m_0 represents the original sugar mass loaded, m_s the equivalent crystal mass sampled, and V_w the water volume.

$$c = \frac{\left(m_0 - \frac{m_s V_{sol}}{10}\right)}{V_w} = \frac{m_0 - m}{V_w} \tag{3}$$

The third distribution moment (volume of crystals/volume of solution) was determined with Eq. (4) where m represents the total crystal mass transferred from the liquid to the solid phase, ρ the crystal density (1.588 g/cm^3) and V_{sol} the solution volume (2691 cm^3).

$$M_3 = \frac{m}{\rho V_{sol}} \tag{4}$$

The CDS measurements obtained with the MasterSizer provided information on the crystal distributions dimensions related to: volume D_{43}, area D_{32}, length D_{21} and number D_{10} per volume of solution. These measurements and distribution moment three were used to evaluate the other distribution moments M_2, M_1 y M_0, using eqs, (5)-(7).

$$M_2 = \frac{M_3}{D_{32}} \tag{5}$$

$$M_1 = \frac{M_2}{D_{21}} \tag{6}$$

$$M_0 = \frac{M_1}{D_{10}} \tag{7}$$

Moments zero, one, and two corresponded to the number of crystals (N), the total length (L), and the total area (A) per unit volume of the solution respectively.

Experimental nucleation and growth rates were calculated for each sampling time, k, with eqs. (8)-(9) respectively.

$$B_{k+1} = \frac{M_{0,k+1} - M_{0,k}}{t_{k+1} - t_k} \tag{8}$$

$$G_{k+1} = \frac{D_{43,k+1} - D_{43,k}}{t_{k+1} - t_k} \tag{9}$$

Kinetic parameters were calculated using two commonly used power-law type equations for nucleation, Eq. (10) and growth, Eq. (11) as function of supersaturation (Zhang, *et al*., 2017). Temperature influence was introduced with an Arrhenius like dependency. The effects of sugar viscosity and agitation rate were not including explicitly because it was assumed that these effects were considered globally by the adjusted parameters. In addition, it was assumed that growth was independent of crystal size. Eqs. (10)-(11) included the six kinetic parameters k_{b0} (# crystals/cm^3 min), k_{g0} (cm/min), ΔE_b (J/mol), ΔE_g (J/mol), b and g representing frequency factors, activation energy and supersaturation exponents for nucleation and growth respectively. R is the ideal gas constant (8.3144 J/mol K) and T is the solution

temperature (K). The kinetic parameters as well as the determination coefficient were estimated with the nonlinear parameter estimation procedure cftool of Matlab.

$$B = k_{b0} \exp\left(\frac{-\Delta E_b}{RT}\right) \ln\left(\frac{c}{c_s}\right)^b \tag{10}$$

$$G = k_{g0} \exp\left(\frac{-\Delta E_g}{RT}\right) \ln\left(\frac{c}{c_s}\right)^g \tag{11}$$

3.3 *Specific surface shape factor estimation*

The specific surface shape factor F, is defined as the ratio of the surface shape factor, f_s, and the volume shape factor, f_v. These factors relate the surface area and volume with a characteristic dimension of crystals. Some authors have associated the characteristic length with the crystal second largest dimension (Mullin, 2001; Jones, 2002). Any change in crystal habit produces different surface areas or volumes; therefore, the specific surface shape factor changes too. In this work, an attempt to quantify this modification in crystal habit is done via the evaluation of the specific surface shape factor, F. This factor is determined minimizing the difference between the growth rate profiles evaluated with the measurements given by the Master Sizer (Eq. 9) and the growth rate calculated based on mass flux transferred, Eq. (12).

$$G = \frac{\Delta m F}{3 \Delta t \rho V_{sol} M_2} \tag{12}$$

where Δm represents the mass transferred from the liquid phase to the solid phase in an interval of Δt (minutes). V_{sol} is the volume of the solution, M_2 is the second distribution moment and ρ is the density of the solution (g/cm^3).

On the other hand, the experimental specific shape factors can be calculated with eqs. (13)-(15), where S_c is the crystal surface area, V_c the crystal volume and L the characteristic crystal length.

$$f_s = \frac{S_c}{L^2} \tag{13}$$

$$f_v = \frac{V_c}{L^3} \tag{14}$$

$$F = \frac{f_s}{f_v} = \frac{S_c L}{V_c} \tag{15}$$

4 Results and discussion

4.1 *Effects of RP on crystallization kinetics*

Fig. 2a shows the sugar concentration as function of time for the experiments cooled following natural or linear profiles. Natural cooling profiles generated a faster decrease in sugar concentration than lineal cooling profiles. Experiments with linear cooling profiles lasted longer to reach the steady state concentration corresponding to 40 °C. Experiments E1-E3 reached the equilibrium at 200 minutes while E4-E6 lasted more than 400 minutes. The presence of RP slowed down the concentration deceasing rate. When more RP mass was added the slower decreasing concentration rates were observed.

Fig. 2b shows how the presence of RP induced larger supersaturations values as the initial RP concentration increased. Supersaturation reached maximum values of 1.2182, 1.2754 and 1.3125 for E1-E3 and 1.1137, 1.1546 and 1.1787 for E4-E6. Natural cooling profile generated bigger maximum supersaturation values than those obtained with linear cooling profiles. Fig. 2c shows the overall effect of the presence of RP on the mass transferred from the liquid phase to the solid phase. It was observed that increasing the initial concentration of RP increased the time at which crystals appeared. For natural cooled experiments, crystals appeared after 20, 30 and 60 minutes for pure, low and high RP initial concentration respectively. A similar trend was shown for experiments cooled with linear cooling profiles (100, 130 and 150 minutes for pure, low and high RP initial concentration respectively).

Figs. 2d-2e show how an increment in the initial RP concentration inhibited nucleation and growth rates. Nucleation maximum values (# nuclei/cm^3 min) were 46560, 28939 and 20217 for experiments E1-E3 and 31109, 27809 and 25728 for experiments E4-E6. It was cleared that nucleation appeared up to the required supersaturation was achieved. Mersmann and Kind (1988) reported values for nucleation between 25000 and 420 000 # nuclei/ cm^3 min in the range of supersaturation from 1.05 to 1.50. In the same way, maximum growth rates values (cm/min) for experiments E1-E6 were 1.7043 $\times 10^{-3}$, 9.1699 $\times 10^{-4}$, 4.0013 $\times 10^{-4}$, 2.9504 $\times 10^{-4}$, 2.2228 $\times 10^{-4}$ and 1.9561 $\times 10^{-4}$. The bigger growth rates produced larger crystals in experiments E1-E3 that those obtained in experiments E4-E6, as shown on Fig. 2f.

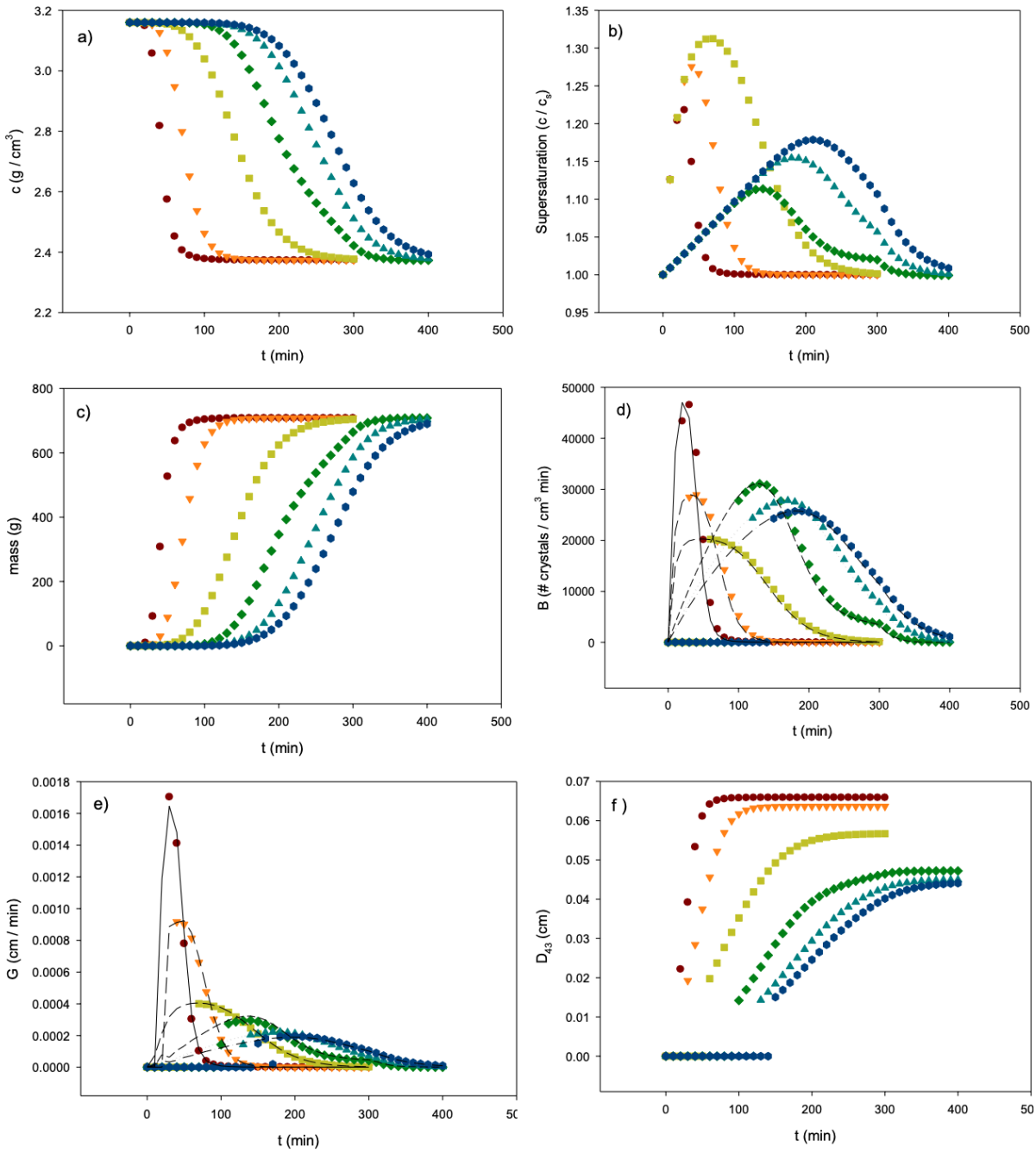

Fig. 2. Experimental results for a) concentration, b) supersaturation, c) mass, d) nucleation rate, e) grow rate and f) D43. Experimental data: ● E1, ▼ E2, ■ E3, ◆ E4, ▲ E5 and ● E6. Calculated data: — E1, −− E2, – – E3, - - - E4, ⋯ E5 and –·– E6.

Mersmann and Kind (1988) reported a growth rate range between 3 $\times 10^{-4}$ to 6 $\times 10^{-4}$ cm/min for the same supersaturation range. The experimental values obtained in this work for nucleation and growth rates were consistent with the values reported by Mersmann and Kind. In addition, growth rates were maximum for pure sugar experiments and decreased when more RP was added. These results indicated that the presence of RP reduced the crystal growth.

Table 2. Correlated kinetic parameters and coefficients of determination.

	$k_{b0} \times 10^{-9}$ # nuclei/cm^{3}min	b	ΔE_b J/mol	R^2	k_{g0} cm/min	g	ΔE_g J/mol	R^2
E1	1.3528	3.0042	26010	0.9315	5.8626	1.0138	16855	0.9666
E2	1.2770	3.1540	27471	0.9675	2.8004	1.0104	16860	0.9677
E3	1.0864	3.3215	28199	0.9782	0.9852	1.0016	16895	0.9766
E4	1.3274	3.0138	26158	0.9921	1.3563	1.0044	16744	0.9501
E5	1.3037	3.1042	26950	0.9903	1.0521	1.0013	17550	0.9186
E6	1.1679	3.3138	27210	0.9485	0.8957	1.0009	17780	0.9073

Table 2 shows the correlated kinetic parameters for all six experiments. The estimate values for activation energies in presence of RP were higher than those presented in experiments with no RP added. Besides, they showed a tendency to increase when RP initial concentration increased. Larger values of activation energy induced a decrement on the overall rate. Therefore, the presence of RP hindered nucleation and crystal growth. Mullin (2001) reported activation energies for diffusion controlling growth in the range of 10-20 kJ/mol and 20-40 kJ/mol for primary nucleation. The average values found in this study were 17.714 kJ/mol for growth and 26.999 kJ/mol for nucleation.

On the other hand, the exponent g is usually referred as the order of the overall crystallization process. It includes the effects of diffusion from the bulk of the fluid phase to the solid surface and the reaction (integration) of the molecules to the crystal lattice. The mass transfer coefficient involved in the molecular diffusion and the rate constant involved in the molecular integration are extremely difficult to evaluate. Therefore, it is difficult to determine the theoretical value of g. However, if a crystallization process were only diffusion-controlled (one step), the molecular flux could be related to the concentration gradient, dc/dx, and a diffusion coefficient; and the resulting crystal growth equation would be lineal. In this work, the average value of g, including all cases shown on Table 2, was close to one, which could be an indication of diffusion-controlled predominant mechanism. Smythe (1967) reported a diffusion controlled mechanisms for sucrose at temperatures above 40 °C. Regarding to the exponent of the nucleation rate, in this work the average value of b was close to three. Garside and Davey (1980) reported exponent nucleation values up to two for homogeneous nucleation. The exponent increased up to five for heterogeneous nucleation. In this work, the presence of impurities (RP) promoted heterogeneous nucleation. The estimated pre-exponential factors decreased in the presence of RP making nucleation and growth smaller with a tendency to decrease when RP increase. Calculated nucleation and growth rates with the empirical correlations were compared against the values calculated experimentally. Figs. 2d-2e include the calculated values represented as solid continuous lines. The comparisons show a good agreement between experimental and calculated values for B and G. Table 2 shows the coefficients of determination and go from 0.9073 to 0.9921.

4.2 Morphological analysis

Changes in crystal habit are normally produced due to the difference between adsorption energies on the crystal faces. Impurities are usually adsorbed in those surfaces with the lowest adsorption free energy. They cover active sites and reduce the face growing rates (Grases *et al.*, 2000). Fig. 3a shows a typical pure sugarcane crystal. It has a monoclinic shape with eight faces distributed symmetrically into four pairs named: a (100), b (111), c (111) and d (100). Faces named "d" represent the front and back faces. Faces with the same crystallographic direction normally grow at the same rate in pure systems. However, when impurities are present faces do not grow at the same rate. Figure 3b shows a fortified sugar crystal where RP was principally adsorbed into face a'. The growing rates of faces b', and c' were faster than the rates of faces b and c respectively. These differences in growing rates modified the habit of the produced crystals. Fig. 3c shows an image of pure crystals at the end of experiment E1 and Fig. 3d shows an image of the fortified sugar crystals at the end of experiment E3. It can be observed that most of the fortified crystals suffered changes in their morphology.

Using the crystal shown on Fig. 3a, the corresponding surface areas for each face were: a = (400)(155), b = (150)(155), c = (150)(155) and d = (400)(200) + (200)(112). The total crystal surface area was equal to 421,721 μm^2.

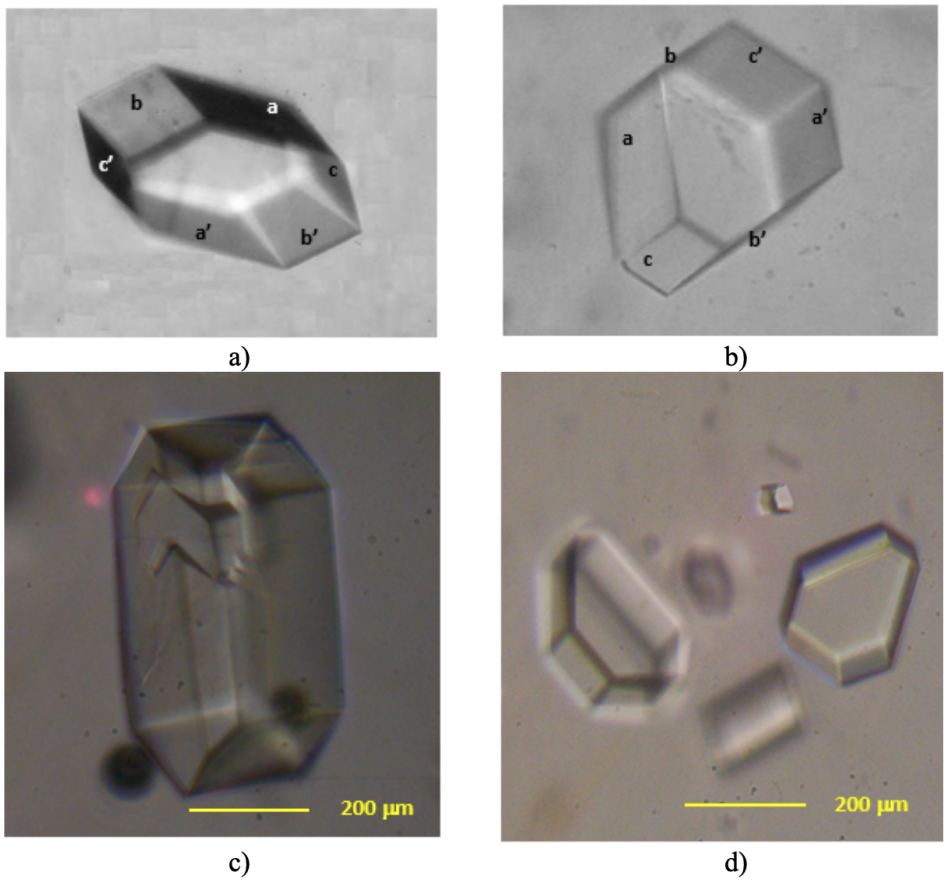

Fig. 3. a) Names designate to the faces of a pure sugar crystal, b) Names designate to the faces of a fortified sugar crystal, c) pure sugar crystal at the end of E1 and d) fortified sugar crystals at the end of E3.

Table 3. Calculated Specific surface shape factors for pure and fortified sugar crystals.

Experiment	Specific surface shape factor F
E1	5.3236
E2	5.1693
E3	4.9979
E4	5.3214
E5	4.8796
E6	4.7047

The crystal volume was equal to 15,865,905 μm^3. The crystal dimensions were length 623 μm, width 200 μm and thickness 155 μm. The experimental specific surface shape factor using the second largest dimension (200 μm) was 5.3160. The same calculations were made for the crystal shown on Fig. 3b. The faces areas were a = (200)(79), b = (75)(70), c = (75)(70), a' = (100)(70), b' = (120)(70), c' = (120)(70), and d = d' =(330+200)(37.4/2) + (330+100)(34.2/2). The total crystal surface area was equal to 82,870 μm^2. The crystal volume was equal to 1,209,965 μm^3. The crystal dimensions were length 330 μm, width 71.7 μm and thickness 70 μm. The experimental specific surface shape factor using the second largest dimension (71.7 μm) was 4.91.

Table 3 shows the specific shape factors evaluated minimizing the differences between Eq. (9) and Eq. (12) for the six experiments. The specific surface shape factors for experiments with no RP (E1 and E4) were 5.3236 and 5.3214 respectively. Those values were in very good agreement with the experimental value of 5.316. When RP initial concentration increased the F factor decreased because the morphological changes induced by the RP. The ratio area/volume of pure crystals (E1 and E4) was equal to 0.02658 μm^{-1} while for E3 it was 0.06849 μm^{-1}. The sugar fortified crystals had larger surface area than the pure ones.

Conclusions

Nucleation and growth rates were successfully determined experimentally for the system sugarcane-water-retinyl palmitate. Kinetic parameters were estimated correlating the experimental data using power-law type relations. The analysis of the kinetic exponents suggested that crystal growth was dominated by a diffusion mechanism and nucleation was dominated by a heterogeneous primary mechanism. Moreover, the results showed that the presence of RP slowed down nucleation and growth rates and induced morphological changes in the habit of the crystals. The evaluation of specific surface shape factors confirmed the habit changes in sugar fortified crystals.

Acknowledgements

The authors sincerely appreciate the financial support of the Consejo Nacional de Ciencia y Tecnología (CONACYT).

References

Bolaños, R.E., Xaca, X.O., Álvarez, R.J. and López, Z.L. (2008). Effect analysis from dynamic regulation of vacuum pressure in adiabatic batch crystallizer using data and image acquisition. *Industrial and Engineering Chemistry Research 47*, 9426-9436. https://doi.org/10.1021/ie071594i

Contreras-Velázquez, L.M. and Hernández-León, R.A. (2005). Solubilidad de la sacarosa en presencia de materias extrañas de caña integral. *Centro Azúcar 32*, 9-13.

Garside, J. and Davey, R.J. (1980). Secondary contact nucleation: Kinetics, growth and scale-up. *Chemical Engineering Communications 4*, 393-399. https://doi.org/10.1080/00986448008935918

Jones, A.G. (2002). *Crystallization Process Systems*, First ed. Oxford: Butterworth-Heinemann, United Kingdom.

Kubota, N. (2001). Effect of impurities on the growth kinetics of crystals. *Crystal Research and Technology 36*, 749-769. https://doi.org/10.1002/1521-4079(200110)36:8/10<749::AID-CRAT749>3.0.CO;2-%23

Medina-Galvan, X.M., Quintana-Hernández, P.A., Reyes-Valadez, J.N. and Fuentes Cortes, L.F. (2020) Determination of kinetic parameters of nucleation and growth for acetylsalicylic acid crystals in ethanol. *Revista Mexicana de Ingeniería Química 19*, 417-428. https://doi.org/10.24275/rmiq/Cat1574

Mersmann, A. and Kind, M. (1988). Chemical engineering aspects of precipitation from solutions. *Chemical Engineering and Technology 11*, 264-276. https://doi.org/10.1002/ceat.270110136

Monaco, L.A. and Rosenberger, F. (1993). Growth an etching kinetics of tetragonal lysozyme. *Journal of Crystal Growth 129*, 465-484. https://doi.org/10.1016/0022-0248(93)90481-B

Mullin, J.W. (2001). *Crystallization*, 4th. Edition. Oxford: Butterworth-Heinemann, United Kingdom.

Qiu, Y. and Rasmuson, A.C. (1994). Estimation of crystallization kinetics from bath cooling experiments. *AIChE Journal 40*, 799-812. https://doi.org/10.1002/aic.690400507

Quintana-Hernández, P.A., Bolaños, E., Saucedo, L. and Miranda, C.B. (2004). Mathematical modeling and kinetic parameter estimation in batch crystallization. *AIChE Journal 50*, 1407-1417. https://doi.org/10.1002/aic.10133

Quintana-Hernández, P.A., Uribe-Martínez, B., Rico-Ramírez, V. and Bolaños-Reinoso, E. (2008). Comparative analysis of power low type and diffusion-integration kinetic equations in batch cooling of sugar cane. *Revista Mexicana de Ingeniería Química 7*, 171-182.

Quintana-Hernández, P.A., Maldonado-Caraza, D., Cornejo-Serrano, M.C. and Villalobos-Oliver, E.E. (2020). Development of a process for sugar fortification with vitamin A. *Revista Mexicana de Ingeniería Química 19*, 1163-1174. https://doi.org/10.24275/rmiq/Proc841

Sánchez-Sánchez, K.B., Bolaños-Reynoso, E. and Urrea-García, G.R. (2017). Analysis of operation conditions for sugar cane batch crystallization based on MSZW mechanistic kinetic models. *Revista Mexicana de Ingeniería Química 16*, 1029-1052. https://rmiq.org/ojs311/index.php/rmiq/article/view/1099

Sánchez-Sánchez, K.B., Bolaños-Reynoso, E., Méndez-Contreras, J.M. and Cerecero-Enriquez, R. (2020). Effects of agitation rates over metastable zone width (MSZW) of concentration for cane sugar crystallization. *Revista Mexicana de Ingeniería Química 19*, 507-520. https://doi.org/10.24275/Proc809

Sarig, S. and Mullin, J.W. (1982). Effect of trace impurities on calcium sulphate precipitation. *Journal of chemical technology and biotechnology 32*, 525-531. https://doi.org/10.1002/jctb.5030320405

Sgualdino, G., Vaccari, G., Mantovani, G. and Aquilano, D. (1996). Implications of crystal growth theories for mass crystallization: Application to crystallization of sucrose. *Progress in crystal growth and characterization of materials 32*, 225-245. https://doi.org/10.1016/0960-8974(96)00002-2

Smythe, B.M. (1967). Sucrose crystal growth. *Australian Journal of Chemistry 20*, 1087-1097. https://doi.org/10.1071/CH9671097

Söhnel, O. and Garside, J. (1992). *Precipitation*, Oxford: Butterworth-Heinemann, United Kingdom.

Ugarte, M., Santana, R., Delgado, I. and Fernández, Y. (1999). Estudio del efecto de impurezas sobre la solubilidad de la sacarosa. *Cuba-Azúcar XXVIII*.

Vavrinecz, G. (1965). *Atlas of Sugar Crystals*. Berlin: Bartens, Germany.

Wey, J.S. (1985). Analysis of bath crystallization processes. *Chemical Engineering Communications 35*, 231 - 252. https://doi.org/10.1080/00986448508911230

Zhang, X.Z., Qian, G. and Zhou, X. (2012). Effects of different organic acids on solubility and metastable zone width of zinc lactate. *Journal of Chemical Engineering Data 57*, 2963-2970. https://doi.org/10.1021/je3006453

Zhang, X.Z., Qian, G. and Zhou, X. (2017). Kinetic modeling on batch-cooling crystallization of zinc lactate: The influence of malic acid. *Journal of Crystal Growth 463*, 162-167. https://doi.org/10.1016/j.jcrysgro.2017.02.023